mol

Initial Sintering Mechanism of 3mol% Yttria doped Zirconia Powder: Effect of Alumina

Koji MATSUI

The sintering behavior of 3 mol% Y_2O_3-doped ZrO_2 powders with and without a small amount of Al_2O_3 was investigated to clarify the effect of Al_2O_3 on the initial sintering mechanism.　The shrinkage behavior of a powder compact was measured under constant rates of heating (CRH).　The shrinkage rate of a powder compact was remarkably increased by a small amount of Al_2O_3.　The activation energies of diffusion at the initial sintering stage were determined by analyzing the shrinkage curves.　The activation energy of a powder compact with Al_2O_3 was lower than that of a powder compact without Al_2O_3.　The diffusion paths of material transport at the initial sintering stage were determined using the analytical equation that is applicable to the CRH data.　This analytical result showed that Al_2O_3 changed the diffusion path from grain boundary (GBD) to volume diffusions (VD).　It is, therefore, concluded that Al_2O_3 enhances the sintering rate because of a decrease in the activation energy with the GBD→VD change at the initial sintering stage.　This enhanced sintering mechanism is reasonably explained by the segregated dissolution of Al_2O_3 at Y-TZP grain boundaries.

Introduction

Yttria-stabilized tetragonal zirconia polycrystal (Y-TZP) has been known as an important structural ceramic, with excellent mechanical properties such as high strength and fracture toughness, and used for products of the optical fiber connector, grinding media, and precision parts.　Hydrolysis is well known as the industrial manufacturing process for Y-TZP powder. The appearance of Y-TZP with the higher characteristic and reliability is desired to spread the zirconia-product market and to propel a new application development. To develop new Y-TZP powder with high quality which is excellent in the sintering characteristic by the hydrolysis process, it is important to analyze the effect of various additives on the sintering mechanism of Y-TZP powder.

So far, the initial stage of sintering on various ceramic powders has been investigated by many researchers, and several sintering-rate equations used for the kinetic analysis at the initial sintering stage have been reported.[1)-9)]　Johnson[1)] has derived the sintering-rate equation (Eq. (1)) that is applied for the initial sintering stage taking into account simultaneous grain-boundary (GBD) and volume diffusions (VD) by assuming the two-sphere shrinkage model.

$$\left(\frac{L}{L_0}\right)^{2.06}\frac{d\left(\frac{\Delta L}{L_0}\right)}{dt}=2.63\frac{\gamma\Omega D_V}{kTa^3}\left(\frac{L}{L_0}\right)^{1.03}+0.7\frac{\gamma\Omega bD_B}{kTa^4}\qquad(1)$$

Here, $\Delta L(=L_0-L)$ is the change in length of the specimen, L_0 the initial length of the specimen, γ the surface energy, Ω the atomic volume, bD_B the GBD coefficient (b is the effective grain-boundary width), D_v the VD coefficient, t the time, T the absolute temperature, k the Boltzmann's constant, and a the

particle radius.

Using Eq. (1), Young and Cutler[2] have derived the sintering-rate equations (Eqs. (2) and (3)) that can quantitatively analyze the densification behavior at the initial sintering stage measured under constant rates of heating (CRH).

$$\frac{d(\Delta L/L_0)}{dT} = \left(\frac{2.14\, bD_{0B}RT}{ka^4 cQ}\right)^{1/3}\left(\frac{Q}{3RT^2}\right)\exp\left(-\frac{Q}{3RT}\right) \quad (2)$$

$$\frac{d(\Delta L/L_0)}{dT} = \left(\frac{5.34\, D_{0V}RT}{ka^4 cQ}\right)^{1/2}\left(\frac{Q}{2RT^2}\right)\exp\left(-\frac{Q}{2RT}\right) \quad (3)$$

Here, Eqs. (2) and (3) are used for GBD and VD, respectively. c is the heating rate (dT/dt), R the gas constant, and Q the activation energy. D_{0B} and D_{0V} represent the constant terms that are given by Eqs. (4) and (5), respectively,

$$bD_B = D_{0B}\exp\left(-\frac{Q}{RT}\right) \quad (4)$$

$$D_V = D_{0V}\exp\left(-\frac{Q}{RT}\right) \quad (5)$$

Using shrinkage data measured by CRH techniques, the Q can be estimated from the slope of the plot of $\ln[T^{5/3}d(\Delta L/L_0)/dT]$ or $\ln[T^{3/2}d(\Delta L/L_0)/dT]$ versus $1/T$ (GBD- or VD-type plot) by assuming GBD or VD. The Qs at the initial sintering stage in yttria-stabilized zirconia and Al_2O_3 were estimated by this analysis method.[2]

Wang and Raj[3, 4] have derived the sintering-rate equation of Eq. (6) used for the quantitative analysis of shrinkage data measured by CRH techniques, noting that the sintering-rate equation in general can be separated into temperature-dependent, grain-size-dependent, and density-dependent quantities:

$$\ln\left[T\left(\frac{dT}{dt}\right)\frac{d\rho}{dT}\right] = -\frac{Q}{RT} + \ln f(\rho)$$
$$+ \ln\left(\frac{C\gamma V^{2/3}}{k}\right) - n\ln d \quad (6)$$

Here, ρ is the density, $f(\rho)$ a function only of density, C a constant, V the molar volume, d the grain size, and

n the grain size power law ($n=3$: VD, $n=4$: GBD). Using shrinkage data measured at different heating rates, the Q can be determined from the slope of the Arrhenius-type plot of $\ln[T(dT/dt)(d\rho/dT)]$ versus $1/T$ at same density, under a constant grain size. The determined Q corresponds to that either for GBD or for VD, because it is very difficult to experimentally determine the GBD- and VD-paths from Eq. (6). The Qs for causing sintering related to Al_2O_3, zirconia (with Y_2O_3), and two-phase Al_2O_3/zirconia (with Y_2O_3) were estimated using Eq. (6).[3, 4]

In this way, the sintering-rate equations that are used for CRH techniques can experimentally determine only the Q for causing diffusion. However, the diffusion path of material transport was experimentally determined by analyzing the isothermal shrinkage process so far because those cannot be determined by CRH techniques.[5, 6] On the other hand, for the research of the zirconia-sintering mechanism, the effects of various additives on the initial sintering stage have not been clarified in previous papers. From the industrial standpoint, it is particularly important to clarify the role of Al_2O_3 which is one of the additives.

In the present study, the author derived the analysis method used for CRH techniques by which not only the Q but the diffusion path of material transport at the initial sintering stage can be determined experimentally, and applied that method in order to examine the initial sintering mechanism of Y-TZP powder with and without a small amount of Al_2O_3. The effect of Al_2O_3 on the initial sintering stage of Y-TZP powder produced by the hydrolysis process (i.e., Tosoh's zirconia process) was determined based on the present analytical results.

Experimental procedure

1　Specimen preparation

3 mol％ (5.2 mass％) Y-TZP powders with and without 0.25 mass％ Al_2O_3 produced by Tosoh's zirconia process (TZ-3Y and TZ-3YE grades, Tosoh,

Table　Chemical composition and characteristic of Y-TZP powder

Specimen	Chemical composition		Powder characteristic	
	Y_2O_3 (mass％)	Al_2O_3 (mass％)	Crystallite size nm	Specific surface area (m²/g)
3Y	5.2	0.005	28	15
3YE	5.2	0.25	28	15

Tokyo, Japan) were used as starting raw materials (Table I).   Both 3Y and 3YE had nearly the same characteristics.   The 3Y and 3YE powders were pressed uniaxially into a disk under 70 MPa.   The resulting powder compacts were sintered at 1100–1500   for 2 h in air (heating rate 100   /h).

2   Density and grain-size measurements

The density of sintered bodies was mainly measured using the Archimedes method.   However, in the case of the sintered bodies with relative densities of < 80   , the density was calculated from the weight and the size. Scanning electron microscopy (SEM; Model S-4500, Hitachi, Tokyo, Japan) was used to measure the average grain sizes of the sintered bodies.   SEM specimens were polished with 3 μm diamond paste, and then thermally etched in air for 1 h at a temperature lower by 50   than the sintering temperature of each specimen. The average grain size was measured by the Planimetric method.[10]

3   Analysis of sintering behavior

The 3Y and 3YE powders were pressed uniaxially into a cylindrical disk under 70 MPa, and afterwards pressed isostatically at 200 MPa.   The size of the resulting powder compacts was 6 mm × 15 mm. The shrinkage of the powder compacts with sintering was measured using a dilatometer (Model DL9700, ULVAC-RIKO, Yokohama, Japan). The shrinkage measurements by CRH techniques were performed in the range from room temperature to 1500   at heating rates of 5, 10, 15, and 20   /min in air.   When the temperature reached 1500   , the CRH measurements were terminated. The dilatometer was calibrated using sapphire as a standard specimen. Using the thermal expansion coefficient of Y-TZP,[11] thermal expansions of the specimens were corrected from the observed shrinkages.   Assuming isotropic shrinkage to powder compact, the density (T) at a given temperature T is given by the following equation[3] :

$$T   \left[\frac{L_f}{L(T)} \right]^3   _f   \qquad 7$$

Here, L_f and $L(T)$ are the final length and the length at a T of the specimen, respectively. $_f$ indicates the final density measured by the Archimedes method. The (T) at a given temperature was calculated using Eq. (7).

Derivation

Using CRH techniques, the concept of the analysis method that is able to determine the diffusion path of material transport at the initial sintering stage is derived as follows.   When Eq. (1) is transformed by the different viewpoint from the derivation procedure that is reported by Young and Cutler,[2] the following sintering-rate equation can be derived by treating separately GBD and VD (Appendix).

$$\ln \left[T \frac{dT}{dt} \frac{d}{dT} \right]   \frac{Q}{RT}   _B \, or \, _V \qquad 8$$

where

$$_B   \ln f_B   \ln \frac{2.14 \, D_{0B}}{k}   4\ln a \qquad 9$$

$$_V   \ln f_V   \ln \frac{5.34 \, D_{0V}}{k}   3\ln a \qquad 10$$

Here, $_B$- and $_V$-terms are used for GBD and VD, respectively. $f_B(\ )$ and $f_V(\ )$ are functions only of density of GBD and VD, respectively.   The Q at the initial sintering stage can be experimentally determined in the same analytical procedure as that reported by Wang and Raj,[3] because the form of Eq. (8) corresponds to that of Eq. (6).   Using the slope S_1 of the Arrhenius-type plot of $\ln[T(dT/dt)(d\ /dT)]$ versus $1/T$ at same density, the Q is expressed by Eq. (11).

$$Q   RS_1 \qquad\qquad 11$$

On the other hand, using the slope S_2 of the GBD- or VD-type plot determined by applying Eqs. (2) and (3), the apparent activation energy (Q/m) is expressed as

$$\frac{Q}{m}   RS_2 \qquad\qquad 12$$

Here, m is the order depending on the material-transport path (m=2: VD, m=3: GBD).   Both Eqs. (11) and (12) are derived using Eq. (1) as the starting equation.   Hence, the Q in Eq. (11) is equal to that in Eq. (12).   Combining Eqs. (11) and (12), one obtains

$$m   \frac{Q}{Q \ m}   \frac{S_1}{S_2} \qquad 13$$

Equation (13) implies that, using both sintering-rate equations of Eqs. (8) and (2)-(3), the diffusion path of material transport at the initial sintering stage can be determined experimentally by CRH techniques. Taking into account the application range of Eq. (1), the present analyses should be performed at the fractional shrinkages of <   4 %   Wang and Raj pointed out that

the exact Q can be estimated under a constant density and particle size.[3] When the fractional shrinkages of <

4 % is satisfied, the influences of density and particle size on the Q and Q/m are negligibly small.

Results and discussion

1 Densification and grain growth

Figure   shows the change of relative densities of 3Y and 3YE with sintering temperature. The relative density of 3YE (including 0.25 mass Al_2O_3) was higher than that of 3Y (including no Al_2O_3) at lower temperatures, and attained 99.6   at 1350 . Figure shows SEM micrographs of the polished and etched surface of 3Y and 3YE sintered at 1300 and 1500 . The grain sizes of both 3Y and 3YE increased as the sintering temperature increased. To analyze quantitatively the grain-growth behavior, the average grain sizes of 3Y and 3YE were determined by the

Planimetric method. As shown in Fig.1, the relationships between the average grain size and the sintering temperature were approximately plotted onto the same curve for 3Y and 3YE.   These experimental results showed that a small amount of Al_2O_3 doped in Y-TZP powder increased the sintering rate remarkably, whereas the grain-growth process was hardly affected at the hold time of 2h in the present sintering profile.

2 Densification behavior at the initial sintering stage

To probe the effect of Al_2O_3 on the sintering rate, the shrinkage behavior of powder compacts of 3Y and 3YE in the course of heating was analyzed by a dilatometric method. Figure 3 shows the change of the shrinkage in the course of 5 /min heating. As seen in Fig. 3(A), the starting temperatures of shrinkage was   1000 , and nearly equal for 3Y and 3YE. Beyond 1150 , the shrinkage of 3YE clearly increased more than that of 3Y.   Using the shrinkage curves in Fig. 3(A), the temperature changes of the relative density ( ) and

Fig.   Changes of relative density and average grain
      size in 3Y and 3YE with sintering temperature.
       and   are 3Y and 3YE, respectively.
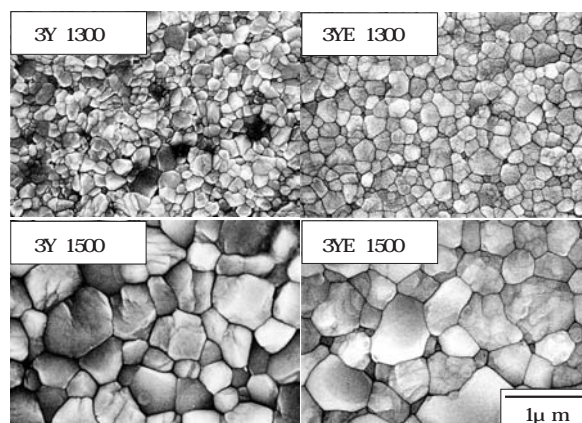
Fig.   SEM micrographs of 3Y and 3YE sintered at
       1300 and 1500
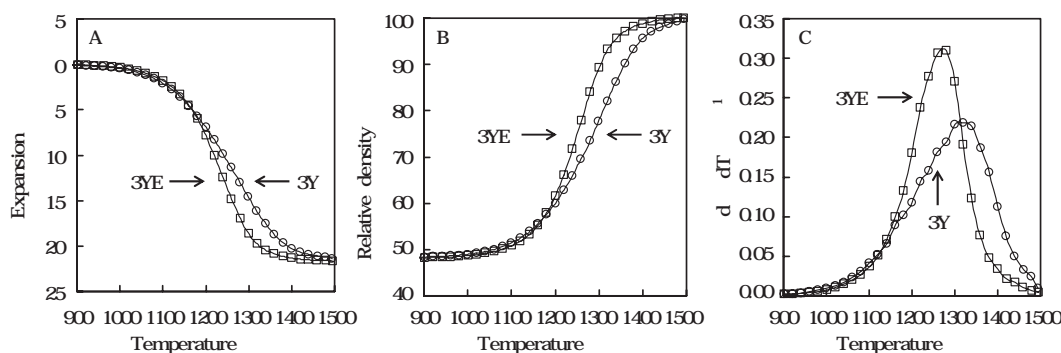
Fig.   Temperature dependence of shrinkage, relative density   , and densification rate d dT of 3Y
       and 3YE in the course of heating 5   min .   and   are 3Y and 3YE, respectively.

the densification rate (d /dT) were determined by Eq.
(8) (Fig. 3(B) and (C)). The   of 3YE was clearly
higher than that of 3Y at temperatures of > 1150 .
The d /dT of 3YE increased more rapidly than that of
3Y when the temperature exceeded 1120 , and the
temperature of peak maximum of the d /dT curve of
3YE shifted to a lower temperature than that of 3Y.
Figure 4 shows the temperature dependence of the d
/dTs of 3Y and 3YE measured at 5-20 /min heating
rates. The d /dT curves of both 3Y and 3YE shifted
to a higher temperature, as the heating rate increased.
The shift of the d /dT curve of 3YE with the increase
in heating rate was greater than that of 3Y. The
present results indicate that Al$_2$O$_3$ doped in Y-TZP
powder increased the d /dT remarkably in the low-
temperature range of < 1300 .

3 CRH shrinkage analysis

To analyze the effect of Al$_2$O$_3$ on the d /dT
quantitatively, the Q at the initial sintering stage was
determined by applying Eq. (8) to the above results.
Equation (8) can be applied in the following way. For
different values of dT/dt of 5, 10, 15, and 20 /min, the
values of T and d /dT at the same were determined,
respectively, and their values were plotted as the
Arrhenius-type plot of T(dT/dt)(d /dT) against 1/T
(Fig. 5). The Q at each was determined from the
slope of the straight line in the Arrhenius-type plot.
The value of $_B$- or $_V$-term was also determined from
the intercept of the straight line in the plot. Here, the
present analysis was performed at the fractional
shrinkages of < 4 (namely, corresponding to the
range of 54 and below), which satisfy the range of the
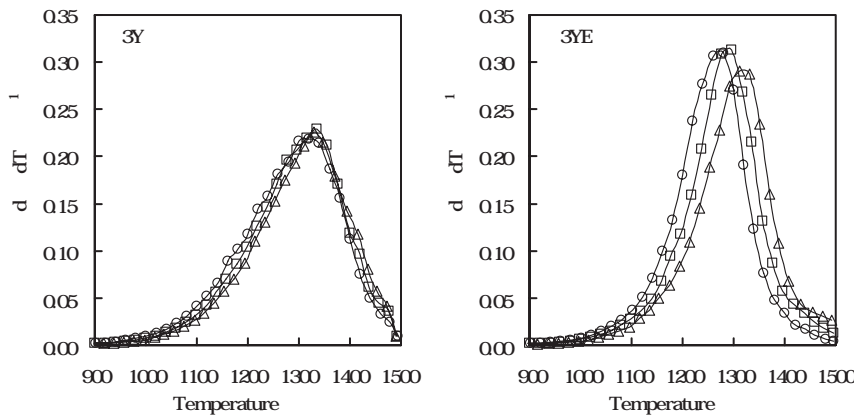
Fig.   Temperature dependence of densification rate d dT of 3Y and 3YE at
various heating rates.   ,   , and   are 5, 10, and 20 min,
respectively. The data measured at a 15 min heating rate were also
obtained in the similar manner.
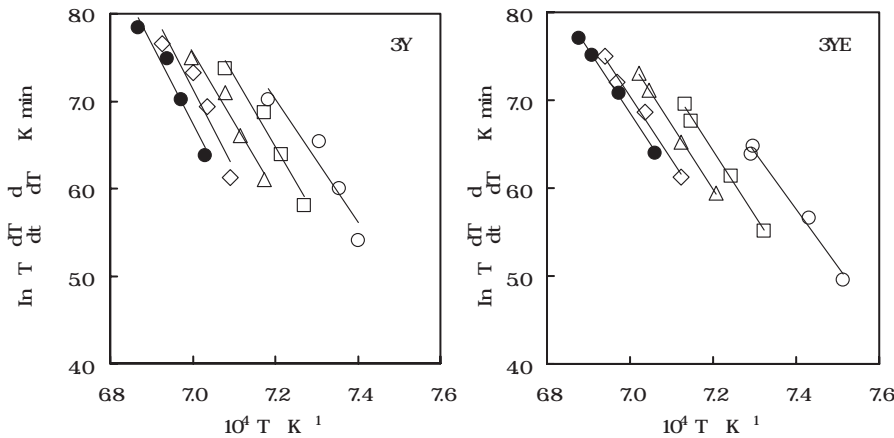
Fig.   Arrhenius type plots for the estimate of activation energies of sintering.
  ,   ,   ,   , and   are 50, 51, 52, 53, and 54 relative densities,
respectively. The data of 50.5, 51.5, 52.5 and 53.5 relative densities were
also obtained in the similar manner.

initial sintering condition without grain growth. Figure 6 shows the Q and $_B$- or $_V$-term in the range of 50-54 . In this range, the Qs of 3YE were lower than those of 3Y (Fig. 6(A)). Determination the average Qs of 3Y and 3YE in the range of 50-54 , the average Q of 3YE was lower than that of 3Y (Table II). Wang and Raj[4] reported that the Q for sintering of zirconia with 2.8 mol (5.0 mass) Y_2O_3 was determined using CRH techniques and by applying Eq. (6) and was estimated to 615± 80 kJ/mol. Compared with that value, the average Q (688 kJ/mol) of 3Y determined by the present analysis is considered to be reasonable. The behaviors of the $_B$- or $_V$-term of 3Y and 3YE also revealed tendencies similar to those of the Qs (Fig. 6(B)). According to Eqs. (9) and (10), the low value of $_B$ or $_V$ of 3YE suggests that the of Y-TZP particles was reduced by Al_2O_3-doping. These analytical results revealed that Al_2O_3 doped in Y-TZP powder decreased the average Q at the initial sintering stage.

It is assumed that the decrease in the average Q appearing as a result of the present of Al_2O_3 occurs by the change of the diffusion path. In order to estimate the order depending on the diffusion path, the values of Q/m of 3Y and 3YE were determined by applying Eqs.

(2) and (3) to the results of the above shrinkage measurements. Equations (2) and (3) were applied in the following way. By assuming both GBD and VD in the same fractional shrinkage range as above, the values of Q/m were determined from the slopes of the GBD- and VD-type plots, respectively. As an example, the GBD- and VD-type plots for 3Y and 3YE at a 5 /min heating rate are shown in Fig. 7. The GBD- and VD-type plots of both 3Y and 3YE revealed nearly linear relations. The values of Q/m for causing GBD and VD were estimated as the average of that determined from the GBD- and VD-type plots of each heating rate, respectively (Table II). Using the values of average Q and Q/m, the orders (m) depending on the diffusion path of material transport at the initial sintering stage were determined by Eq. (13) (Table II). The values of m of GBD and VD of 3Y were both close to 3, and their values of 3YE were both close to 2. Taking into account that the values of m of GBD and VD correspond to 3 and 2, respectively, the diffusion paths of 3Y and 3YE is assigned to GBD and VD, respectively. In previous papers, the author analyzed the initial sintering behavior of Y-TZP powder with and without a small amount of Al_2O_3 by the isothermal shrinkage analysis, and reported that Al_2O_3 changes the diffusion
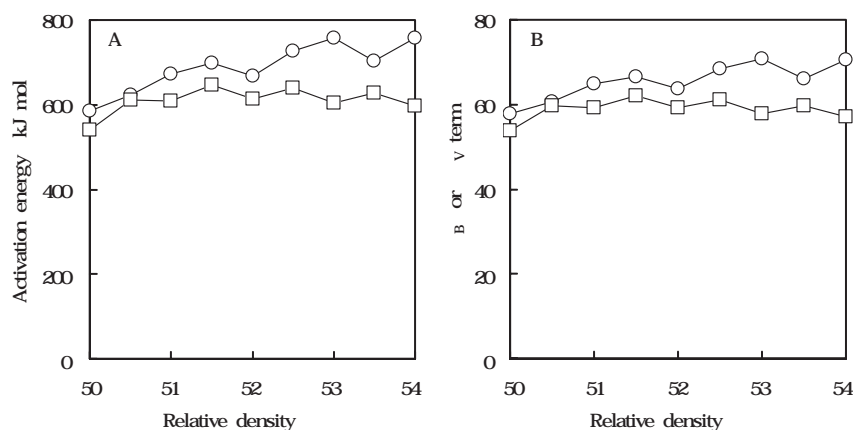
Fig.   Activation energy and $_B$ or $_V$ term of 3Y and 3YE at 50 54 relative densities.   and   are 3Y and 3YE, respectively.

Table   Activation energies, apparent activation energies, and orders depending on diffusion path

Specimen	Activation energy kJ mol		Apparent activation energy kJ mol				Order on diffusion path m	
	Q	Standard deviation	GBD Q m	Standard deviation	VD Q m	Standard deviation	GBD	VD
3Y	688	58	222	5	221	5	3.1	3.1
3YE	605	31	259	4	258	4	2.3	2.3
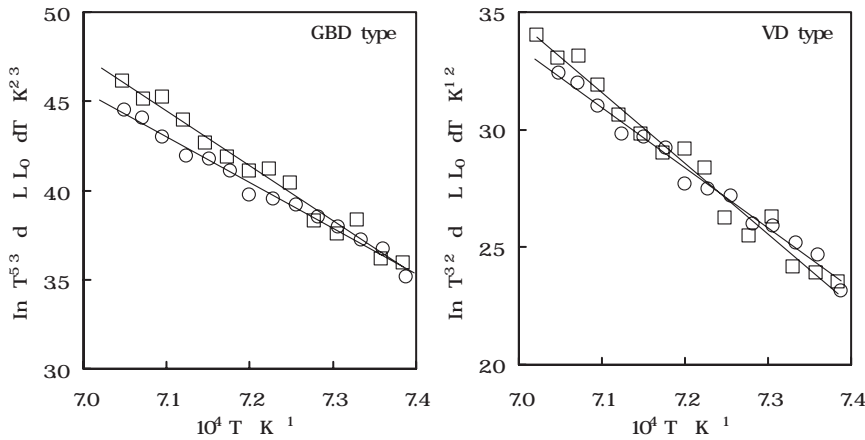
Fig.   GBD and VD type plots of 3Y and 3YE in the course of heating 5   min .
and   are 3Y and 3YE, respectively.

path at the initial sintering stage from GBD to VD.[12-15] The analytical results of 3Y and 3YE agree with these reports.   It is, therefore, clarified that the diffusion path of material transport at the initial sintering stage can be experimentally determined by applying the present analytical method to CRH experiments.

Taking into account the results obtained in the present CRH analysis, it is clarified that the role of Al_2O_3 doped in Y-TZP powder changes the diffusion path at the initial sintering stage from GBD to VD, and the d /dT remarkably enhances because of the decrease in the Q with the GBD   VD change.

4 Al_2O_3 effect

It is generally known for the comparison in the same oxide that the Q for causing GBD is smaller than that for causing VD.   Therefore, the Q for VD of Y-TZP without Al_2O_3 is assumed to be a value of > 688 kJ/mol, because the Q for GBD of 3Y was estimated to 688 kJ/mol by the present CRH analysis.   In the present results, Al_2O_3 changed the diffusion path of material transport at the initial sintering stage from GBD to VD and, contrary to the general tendency above, the Q (605 kJ/mol) for VD of 3YE was smaller than that for GBD of 3Y.   These results evidently exhibit that a small amount of Al_2O_3 directly affects the diffusion path at the initial sintering stage of Y-TZP powder.

Al_2O_3 and ZrO_2 (without Y_2O_3) are known to exhibit very limited mutual solubility (0.1   at 1300   ), and the solubility of Al_2O_3 in ZrO_2 increases as the temperature increases.[16, 17]   Analogizing from these reports, it is assumed that the behavior of the enhanced

d /dT of 3YE relates to the solubility of Al_2O_3 in Y-TZP, and the d /dT increases with increasing amount of dissolved Al_2O_3.   The author has reported that the microstructure development in 3Y and 3YE during sintering which was analyzed using high-resolution electron microscopy and nanoprobe X-ray energy dispersive spectroscopy techniques.[18]-[21]   In these analytical results, it has been showed that no amorphous layer exists along the grain-boundary faces in 3Y and 3YE, but Y^{3+} ions segregate at the grain boundaries over a width of   10 nm, and in 3YE, Al^{3+} ions also segregate at grain boundaries over a width of

6 nm.   As shown in Fig. 8, in the 3YE sintered at 1100   , Al^{3+} ions have already segregated at grain boundaries, and the segregation of Al^{3+} ions increases with increasing sintering temperature.[20]   Taking into account these reports, it is concluded that as the result of segregated dissolution of Al_2O_3 at Y-TZP grain boundaries, the diffusion path changes to VD and the Q for VD is lower than that for GBD of Y-TZP without Al_2O_3.   Because the decrease of $_V$-term of 3YE in Fig. 6(B) indicates a decrease in the   of Y-TZP powder, the segregated dissolution of Al_2O_3 at Y-TZP grain boundaries may be considered.

Conclusions

In the present study, the author derived the analytical method used for CRH techniques by which the diffusion path at the initial sintering stage can be determined experimentally.   To substantiate the validity of the derived analysis method, the initial
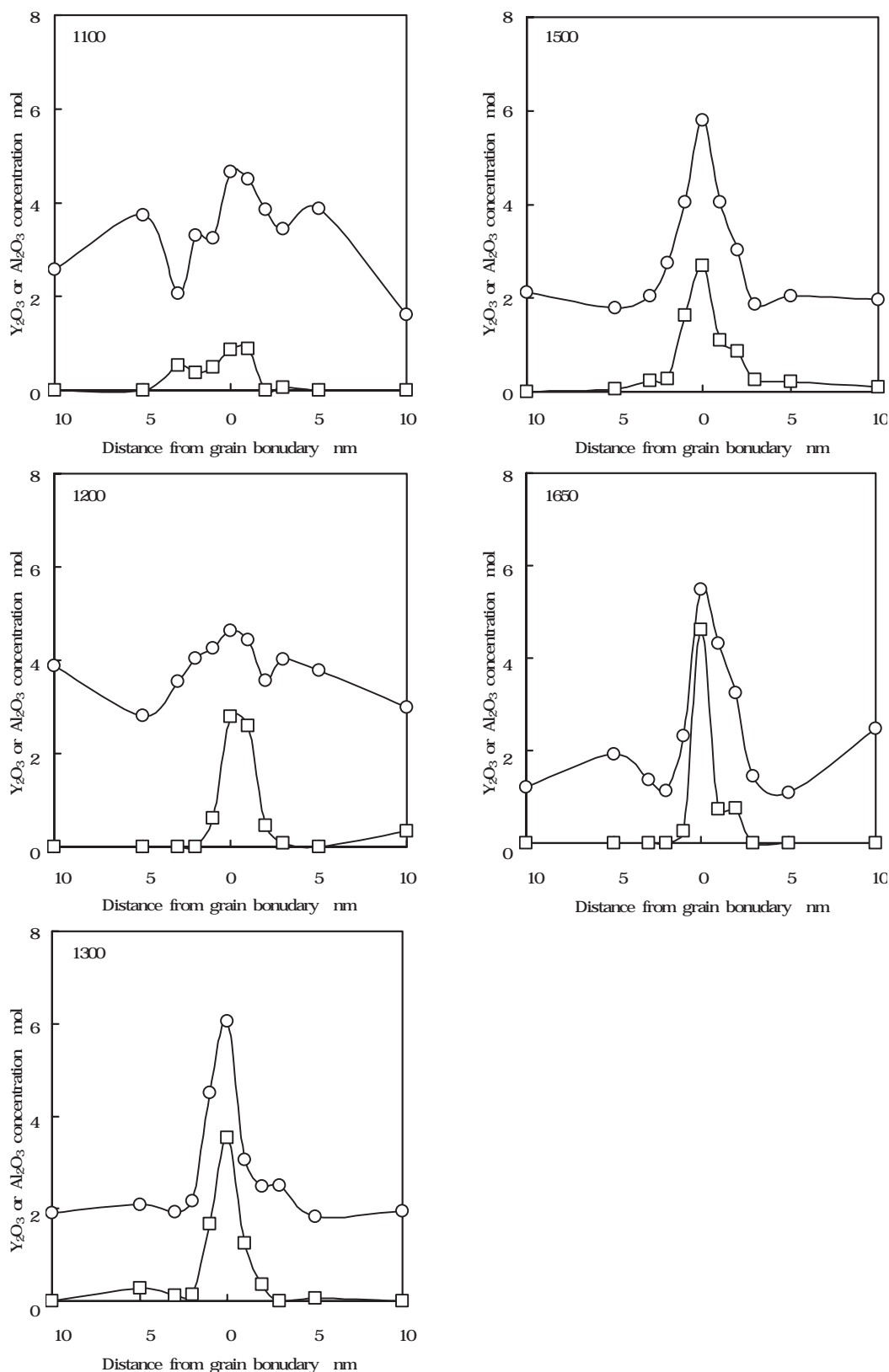
Fig.   Y and Al concentration profiles across the grain boundaries in 3YEs sintered at 1100 1650 .[20]
              and   indicate Y and Al, respecitively.

sintering mechanisms of Y-TZP powder with and
without a small amount of Al_2O_3 were examined by
applying this method.   The following conclusions were

obtained:

1 A small amount of Al_2O_3 doped in Y-TZP powder
    enhanced the sintering rate remarkably, whereas

the grain-growth process was hardly affected at the hold time of 2 h in the present sintering profile. CRH measurements revealed that Al_2O_3 doped in Y-TZP powder remarkably increased the $d\rho/dT$ in the low-temperature range of $< \sim 1300$.

2 By applying the present analytical method to the CRH shrinkage curves, it is clarified that the Al_2O_3 effect on the initial sintering stage changes the diffusion path from GBD to VD, and remarkably increases the $d\rho/dT$ because of the decrease in the Q with the GBD $\rightarrow$ VD change. This enhanced sintering mechanism is reasonably explained by the segregated dissolution of Al_2O_3 at Y-TZP grain boundaries.

3 The present analytical method derived based on the sintering kinetics at CRH is very useful for determination of the diffusion mechanism at the initial sintering stage of ceramic powders.

Appendix

Eqs. (8)-(10) can be derived as follows, using Eq. (1) reported by Johnson.[1] If the isothermal shrinkage process proceeds only at GBD, Eq. (1) can be expressed as Eq. (A1).

$$\left(\frac{\Delta L}{L_0}\right)^{2.06} d\left(\Delta L\,L_0\right) = \frac{0.7\gamma bD_B}{kTa^4}dt \qquad \text{A1}$$

Substituting the differential equation of heating rate (namely, $dt = dT/c$) into Eq. (A1) and eliminating dt, one obtains the following equation.

$$\left(\frac{\Delta L}{L_0}\right)^{2.06} d\left(\Delta L\,L_0\right) = \frac{0.7\gamma bD_B}{kTa^4 c}dT \qquad \text{A2}$$

Substituting Eq. (4) into Eq. (A2) (i.e., eliminating bD_B) becomes

$$\left(\frac{\Delta L}{L_0}\right)^{2.06} d\left(\Delta L\,L_0\right) = \frac{0.7\gamma D_{0B}}{ka^4 c}$$
$$\frac{\exp\left(-\,Q\,RT\right)}{T}dT \qquad \text{A3}$$

Integrating Eq. (A3) at the ranges of $\Delta L/L_0=0 \sim \Delta L/L_0$ and $T=T_0 \sim T$ results in

$$\left(\frac{\Delta L}{L_0}\right)^{3.06} = \frac{2.14\gamma D_{0B}}{ka^4 c}\int_{T_0}^{T}\frac{\exp\left(-\,Q\,RT\right)}{T}dt \qquad \text{A4}$$

Here, T_0 is a room temperature. The differentiation of Eq. (A4) with respect to T gives

$$\frac{d}{dT}\left(\frac{\Delta L}{L_0}\right)^{3.06} = \frac{2.14\gamma D_{0B}}{ka^4 c}\frac{\exp\left(-\,Q\,RT\right)}{T} \qquad \text{A5}$$

Since the $\Delta L/L_0$ is correlated with the density, as shown in Eq. (A6), $\left(\Delta L/L_0\right)^{3.06}$ can be expressed as the function of density, $F_B(\rho)$.

$$\left(\frac{\Delta L}{L_0}\right)^{3.06} = F_B(\rho) \qquad \text{A6}$$

Differentiating Eq. (A6) with respect to ρ, one obtains Eq. (A7).

$$\frac{d}{d\rho}\left(\frac{\Delta L}{L_0}\right)^{3.06} = \frac{d}{d\rho}F_B(\rho) = F'_B(\rho)$$
$$d\left(\frac{\Delta L}{L_0}\right)^{3.06} = F'_B(\rho)\,d\rho \qquad \text{A7}$$

Combining Eqs. (A7) and Eq. (A5) gives

$$Tc\frac{d\rho}{dT} = \frac{1}{F'_B(\rho)}\frac{2.14\gamma D_{0B}}{ka^4}\exp\left(-\,\frac{Q}{RT}\right) \qquad \text{A8}$$

Here, when $F'_B(\rho)$ is formally placed as $1/f_B(\rho)$ (namely, $F'_B(\rho) = 1/f_B(\rho)$), Eq. (A8) can be expressed by Eq. (A9).

$$Tc\frac{d\rho}{dT} = f_B(\rho)\frac{2.14\gamma D_{0B}}{ka^4}\exp\left(-\,\frac{Q}{RT}\right) \qquad \text{A9}$$

Substituting $c = dT/dt$ into Eq. (A9) and taking logarithms, one obtains

$$\ln\left(T\frac{dT}{dt}\frac{d\rho}{dT}\right) = -\frac{Q}{RT} + \psi_B \qquad 8$$

where

$$\psi_B = \ln f_B(\rho) + \ln\frac{2.14\gamma D_{0B}}{k} - 4\ln a \qquad 9$$

If the isothermal shrinkage process proceeds only at VD, Eq. (1) can be expressed as Eq. (A10)

$$\left(\frac{\Delta L}{L_0}\right)^{1.03} d\left(\Delta L\,L_0\right) = \frac{2.63\gamma D_V}{kTa^3}dt \qquad \text{A10}$$

Substituting $dt = dT/c$ and Eq. (5) into Eq. (A10) results in

$$\left(\frac{\Delta L}{L_0}\right)^{1.03} d\left(\Delta L\,L_0\right) = \frac{2.63\gamma D_{0B}}{ka^3 c}$$
$$\frac{\exp\left(-\,Q\,RT\right)}{T}dT \qquad \text{A11}$$

Integrating and differentiating Eq. (A11) at the same conditions as above result in

$$\frac{d}{dT}\left(\frac{\Delta L}{L_0}\right)^{2.03} = \frac{5.34\gamma D_{0B}}{ka^3 c}\frac{\exp\left(-\,Q\,RT\right)}{T} \qquad \text{A12}$$

Here, $\left(\Delta L/L_0\right)^{2.03} = F_V(\rho)$. The differentiation of this equation with respect to ρ leads to

$$d\left(\frac{\Delta L}{L_0}\right)^{2.03} = F'_V(\rho)\,d\rho \qquad \text{A13}$$

Substituting Eq. (A13) into Eq. (A12) results in

$$Tc\frac{d\rho}{dT} = f_V(\rho)\frac{5.34\gamma D_{0V}}{ka^3}\exp\left(-\,\frac{Q}{RT}\right) \qquad \text{A14}$$

Here, $f_V(\rho) = 1/F'_V(\rho)$. Substituting $c = dT/dt$ into Eq. (A14) and taking logarithms, one obtains

$$\ln T \quad \frac{dT}{dt} \quad \frac{d}{dT} \qquad \frac{Q}{RT} \quad _v \qquad\qquad 8$$

where

$$_v \quad \ln \quad f_V \qquad \ln \frac{5.34 \quad D_{\alpha v}}{k} \qquad 3\ln a \quad 10$$

Acknowledgement

The author would like to express his sincere thanks to Professor Junichi Hojo, Kyushu University, for his valuable advice in this work.

Reference

D.L.Johnson, *J.Appl.Phys.*, 40(1), 192(1969).

W.S.Young and I.B.Cutler, *J.Am.Ceram.Soc.*, 53(12), 659(1970).

J.Wang and R.Raj, *J.Am.Ceram.Soc.*, 73(5), 1172(1990).

J.Wang and R.Raj, *J.Am.Ceram.Soc.*, 74(8), 1959(1991).

D.L.Johnson and I.B.Cutler, *J.Am.Ceram.Soc.*, 46(11), 541(1963).

D.L.Johnson and I.B.Cutler, *J.Am.Ceram.Soc.*, 46(11), 545(1963).

Y.Moriyoshi and W.Komatsu, *J.Am.Ceram.Soc.*, 53(12), 671(1970).

H.Su and D.L.Johnson, *J.Am.Ceram.Soc.*, 79(12), 3211(1996).

T.Ikegami, *J.Ceram.Soc.Jpn* 106(5), 456(1998).

10 T.Yamaguchi, *Ceramics Jpn*, 19(6), 520(1984).

11 Edited by T.Yamaguchi and H.Yanagita, "*Enjiniaringu Seramikkusu,*" ; pp.22-25, Gihodo, Tokyo, 1984.

12 K.Matsui, N.Ohmichi, M.Ohgai, T.Yamakawa, M.Uehara, N.Enomoto, and J.Hojo, *J.Ceram.Soc.Jpn.*, 112(5, Supp. 112-1, PacRim5 Special Issue), S343(2004).

13 K.Matsui, N.Ohmichi, M.Ohgai, N.Enomoto, and J.Hojo, *J.Am.Ceram.Soc.*, 88(12), 3346(2005).

14 K.Matsui, A.Matsumoto, M.Uehara, N.Enomoto, and J.Hojo, *J.Am.Ceram.Soc.*, 90(1), 44(2007).

15 K.Matsui, K.Tanaka, T.Yamakawa, M.Uehara, N.Enomoto, and J.Hojo, *J.Am.Ceram.Soc.*, 90(2), 443(2007).

16 S.N.B.Hodgson, J.Cawley, M.Clubley, *J. Mater. Process. Tech.*, 92-93, 85(1999).

17 Edited by H.M.Ondik and H.F.McMurdie, "*Phase Diagrams for Zirconium and Zirconia Systems,*" ; p63(Fig. Zr-084), Am.Ceram.Soc., Ohio, 1998.

18 K.Matsui, H.Horikoshi, N.Ohmichi, M. Ohgai, H.Yoshida, and Y.Ikuhara, *J.Am.Ceram.Soc.*, 86(8), 1401(2003).

19 K.Matsui, N.Ohmichi, M.Ogai, H.Yoshida, and Y.Ikuhara, *J.Ceram.Soc.Jpn*, 114(3), 230(2006).

20 K.Matsui, N.Ohmichi, M.Ogai, H.Yoshida, and Y.Ikuhara, *J.Mater.Res*, 21(9), 2278(2006).

21 K.Matsui, H.Yoshida, and Y.Ikuhara, *Mater. Sci. Forum*, 558-559, 921(2007).

19

Koji MATSUI

61　4　1